

## DESCRIPTION OF ROTATIONAL BANDS AT HIGH SPINS IN RARE EARTH EVEN-EVEN NUCLEI USING MULTI PARAMETER EXPRESSION FOR THE KINEMATIC MOMENT OF INERTIA

**M.M. Sirag**

*Physics Department, Girls College, Ain Shams University, Cairo, Egypt.*

*Rec. 24/7/2005*

*Accept. 24/7/2006*

Since the graph of moment of inertia versus the square of rotational frequency amplifies the relevant details of the nuclear rotational spectra, it should be preferable to use the moment of inertia rather than the energy. A multi-parameter polynomial in even power of mean angular momentum for the kinematical moment of inertia is considered to analyze the yrast state rotational bands of even-even deformed nuclei in the rare-earth region including high spin states. The optimized expansion parameters have been deduced by using a computer simulated search program in order to obtain a minimum root mean square deviation of the calculated kinematical moment of inertia from the experimental ones. The multi-parameter expression was used to investigate the mechanism of backbending and upbending in nuclear moments of inertia. A systematic study of the level structure up to spin  $20^+$  of eight selected nuclides including soft as well as good rotors and exhibit backbending or upbending are performed.

**Keywords:** *Rotational bands, high spins, rare-earth nuclei.*

### INTRODUCTION

Since the discovery [1] of backbending at high spins in the ground state rotational bands (GSRB) of even-even rare earth nuclei  $^{160}\text{Dy}$  and  $^{162}\text{Er}$ , this effect has been extensively studied in many even-even nuclei. The sudden decrease of the rotational frequency and anomalous increasing in the moment of inertia has been found to occur in many deformed nuclei of the rare earth region at spins of about  $14^+$ . It has also been observed in other regions of the nuclide chart. The word backbending refers to the phenomenon in which a plot of twice the moments of inertia versus the square of rotational frequency, for the various spin states has an S-shaped form.

A number of explanations for backbending have been given. One of these explanations predated the experimental observations by eleven years, and is known as the Mottelson-Valatin effect or the Coriolis anti-pairing effect [2]. This explanation refers to a coherent collapse of the pairing correlations in the nucleus due to increasing the Coriolis force as the system rotates more rapidly. This causes a phase transition from the normal superfluid state to one in which the nucleon pairs have been coherently broken by the Coriolis force.

An alternative explanation proposed shortly after the experiments by F.S. Stephens and R. Simon was called the rotation-alignment model (RAL) [3, 4], in which it is suggested that only one pair of  $I_{13/2}$  neutrons is broken by the Coriolis force. The angular momentum from this pair is then aligned with that of the rotating core to produce a band (super band) which crosses the ground-state band at the backbend, and the larger spin values becomes the yrast band. The RAL model has enjoyed considerable success, particularly in identifying the relationship between backbending in neighbouring odd and even nuclei. The first sharp backbending observed in deformed rare-earth nuclei was understood as the crossing between the ground state band and a high-j two quasiparticle band [5-7].

Other models involving centrifugal shape changes [8-10] or generalized moment of inertia changes have been proposed. The larger moment of inertia is due to a second minimum or inflection point in the deformation surface. Also the nature of backbending has been explained in terms of pairing vibration.

Recently, a new interest in the backbending phenomenon has arisen through a series of experiments for nuclei in the  $A \sim 180$  region [11-14]. It is expected that the backbending in this region is caused by the three-bands crossing, i.e., the ground ( $g^-$ ), super ( $s^-$ ) and tilt ( $t^-$ ) bands [14, 15], unlike the backbending caused by the two-bands crossing of the  $g^-$  and  $s^-$  bands [3] in light rare-earth nuclei. The  $t^-$  band was proposed as tilted rotational band [16].

There have been systematic investigations over chains of isotopes, e.g., the Dy isotopes [17, 18] and Yb isotopes [19]. Experimental results show that the degree of backbending depends on the Coriolis response and the spacing of the single particle levels near the Fermi surface. For example, while a sharp backbending was found in  $^{170}\text{Yb}$ , no backbending in  $^{172}\text{Yb}$  and  $^{174}\text{Yb}$  was found. In odd-A nuclei it has been noted that the nuclear moment of inertia depends on the blocking effects of the unpaired nucleon, which lead to a large fluctuation in the odd-even difference in moment of inertia [20].

In this paper a single expression for the kinematic moment of inertia was proposed to investigate the mechanism of backbending and upbending in some

selected rare-earth nuclides. The paper is organized as follows: In the next section the proposed formula is given. In the section entitled “Aligned Angular Momentum and Routhian” the alignment and Routhian are discussed. In the last section numerical calculations and discussions are presented.

### OUTLINE OF THE METHOD

The ground-state rotational bands of even-even nuclei in the rare-earth region for spins  $I \sim 20$  show an anomalous behavior in the nuclear rotational motion for large values of angular momenta. Usually the rotational frequency  $\hbar\omega$  and the moment of inertia  $J^{(1)}$  are deduced from the transition energy by defining:

$$\hbar\omega = \frac{dE(I)}{d\hat{I}}, \quad \hat{I} = [I(I+1)]^{1/2} \quad (1)$$

so that for discrete states

$$\hbar\omega = \frac{\Delta E(I)}{[I(I+1)]^{1/2} - [(I-2)(I-1)]^{1/2}} \quad (2)$$

$$\cong \frac{1}{2} \Delta E(I) \quad (3)$$

and

$$\frac{J^{(1)}}{\hbar^2} = \frac{1}{2} \left[ \frac{dE(I)}{d\hat{I}^2} \right]^{-1} \quad (4)$$

$$= \frac{2I-1}{\Delta E(I)} \quad (5)$$

where

$$\Delta E(I) = E(I) - E(I-2) \quad (6)$$

is the observed energy difference between neighboring levels.

In the absence of detailed microscopic calculations attempts have been made to describe the dependence of the moment of inertia  $J^{(1)}$  on the square of rotational frequency  $\hbar^2\omega^2$  phenomenologically. At low spins a very successful description is the variable moment of inertia (VMI) model [21, 22] which give a simple linear

dependence of  $J^{(1)}$  and  $\hbar^2\omega^2$ . For large values of spins,  $J^{(1)}$  does not remain a single-valued function of  $\hbar^2\omega^2$ ,  $J^{(1)}$  as a function of  $\omega$  exhibits a strange behavior. The values of  $J^{(1)}$ , which usually increases with increasing  $\omega$ , begin to decrease at a certain moment of inertia, and then again increases, giving the S-shaped curve. So for spin region  $I \leq 30$ , one can reproduce the features of the spectra by modifying the kinematic moment of inertia.

In this paper, under adiabatic approximation of an axially symmetric normal deformed nucleus, the kinematic moment of inertia of the states of a rotational band with mean angular momentum  $I_m$  may be expressed quite generally in the form:

$$J^{(1)} = J_1 + \sum_{n=1} \left[ A_{2n} \hat{I}_m^{(n-1)\ell+2} + A_{2n+1} \hat{I}_m^{n\ell} \right] \quad (7)$$

$$n = 1-6; \quad \ell = 4-12$$

with

$$\hat{I}_m = \frac{1}{2} \left\{ [I(I+1)]^{1/2} + [(I-2)(I-1)]^{1/2} \right\} \quad (8)$$

where

$$A_{2n} = (-J_0)^{n-1} J_2$$

$$A_{2n+1} = (-J_0)^{n-1} J_3$$

$J_0, J_1, J_2, J_3$  and  $\ell$  are the parameters for the ground state rotational band.

### ALIGNED ANGULAR MOMENTUM AND ROUTHIAN

Following the cranked shell model (CSM) [5, 6] the experimental frequency within a rotational band at the mean angular momentum  $I_m$  can be calculated from the transition energies  $\Delta E_\gamma(I \rightarrow I-2)$  via:

$$\hbar\omega(I_m) = \frac{dE(I_m)}{dI_x(I_m)} \quad (9)$$

$$= \frac{E(I_{m+1}) - E(I_{m-1})}{I_x(I_{m+1}) - I_x(I_{m-1})} \quad (10)$$

$$\cong \frac{1}{2} E_\gamma(I \rightarrow I-2), \text{ valid for } I \gg K. \quad (11)$$

$I_x$  is the angular momentum along the rotation axis (x-axis) and is given by

$$I_x(I_m) = \left[ \left( I_m + \frac{1}{2} \right)^2 - K^2 \right]^{1/2} \quad (12)$$

where  $K$  is the projection of  $I$  on the nuclear symmetry axis ( $z$ -axis).

In order to deduce the alignment of the super band, the angular momentum due to the reference collective motion has to be subtracted from  $I_x$ . The reference taken according to the Harris formula is used [5].

$$I_x^{\text{ref}}(\omega) = \theta_0 \omega + \theta_1 \omega^3 \quad (13)$$

where  $\theta_0$  and  $\theta_1$  are the Harris parameters [23].

Therefore, the aligned angular momentum  $i$  of the excited band relative to the ground configuration at a certain  $\omega$  is

$$i(\omega) = I_x(\omega) - I_x^{\text{ref}}(\omega) \quad (14)$$

In order to compare the eigenstates of the Routhian (excitation energy in rotating frame) with experimental level energies, the excitation energy has to be calculated within the rotating frame.

$$E'(I_m) = \frac{1}{2} [E(I_{m+1}) + E(I_{m-1})] - \omega(I_m) \cdot I_x(I_m) \quad (15)$$

where  $\omega I_x$  is the energy of rotation in pure rotator.

To obtain the quasi particle contribution, the collective part must be subtracted

$$e'(\omega) = E'(\omega) - E'^{\text{ref}}(\omega) \quad (16)$$

where  $e'$  is the energy in the rotating frame relative to the ground band.  $E'^{\text{ref}}$  can be calculated as

$$E'^{\text{ref}}(\omega) = -\int I_x^{\text{ref}}(\omega) d\omega \quad (17)$$

$$= -\frac{1}{2} \omega^2 \theta_0 - \frac{1}{4} \omega^4 \theta_1 + \frac{1}{8\theta_0} \quad (18)$$

The constant of integration  $1/8\theta_0$  has been added to assume approximately vanishing  $E'^{\text{ref}}(0)$  at  $I = 0$ .

## NUMERICAL CALCULATIONS AND DISCUSSIONS

For each nucleus the optimized five parameters  $J_0$ ,  $J_1$ ,  $J_2$ ,  $J_3$  and  $l$  of the model in question are fitted to reproduce the calculated kinematic moment of inertia from the observed energies. The procedure is repeated for several trial values of the parameters by using a computer simulation search program. The best parameters minimize the root-mean square (rms) deviation

$$\chi = \left[ \frac{1}{N} \sum_{i=1}^N (J_{\text{cal}}^{(i)} - J_{\text{exp}}^{(i)})^2 \right]^{1/2} \quad (19)$$

The calculated kinematical moment of inertia is proposed in eq.(7).

The optimized parameters of the model for the selected eight nuclei  $^{158, 160}\text{Dy}$ ,  $^{162}\text{Er}$ ,  $^{168, 170}\text{Yb}$  and  $^{172, 176}\text{Hf}$  are listed in Table 1.

**Table 1.** The optimized parameter values for the GSRB's of the selected even-even nuclides in the rare-earth region using the proposed formula for the kinematic moment of inertia.

Nucleus	$J_0$	$J_1$ ( $\hbar^2 \text{MeV}^{-1}$ )	$J_2$ ( $\text{MeV}^{-1}$ )	$J_3$ ( $\text{MeV}^{-1}$ )	$l$
$^{158}\text{Dy}$	$3 \times 10^{-11}$	31.07	$9.321 \times 10^{-2}$	$8.388901 \times 10^{-10}$	8
$^{160}\text{Dy}$	$3 \times 10^{-13}$	34.84	$6.68928 \times 10^{-2}$	$9.406801 \times 10^{-12}$	10
$^{162}\text{Er}$	$4 \times 10^{-15}$	29.87	$8.0649 \times 10^{-2}$	$1.43376 \times 10^{-13}$	12
$^{168}\text{Yb}$	$1 \times 10^{-6}$	34.15	$8.63995 \times 10^{-2}$	$-1.5026 \times 10^{-5}$	4
$^{170}\text{Yb}$	$3 \times 10^{-11}$	35.65	$4.81275 \times 10^{-2}$	$9.6255 \times 10^{-10}$	8
$^{172}\text{Hf}$	$3 \times 10^{-6}$	31.71	$8.40315 \times 10^{-2}$	$1.9026 \times 10^{-5}$	4
$^{174}\text{Hf}$	$1 \times 10^{-6}$	32.95	$7.80915 \times 10^{-2}$	$-8.027298 \times 10^{-13}$	4
$^{176}\text{Hf}$	$3 \times 10^{-6}$	33.94	$6.17708 \times 10^{-2}$	$-2.036396 \times 10^{-6}$	4

The calculated results for the ground state rotational bands are given systematically in Tables 2.-9.

**Table 2.** Calculated energies  $E(\text{keV})$ , kinematic moment of inertia  $J^{(1)}(\hbar^2\text{MeV}^{-1})$  and square of nuclear rotational frequency  $\hbar^2\omega^2(\text{MeV}^2)$  predicted with the parameters listed in Table 1. for  $^{158}\text{Dy}$  and comparison with experiment.

E (keV)		$I^\pi$	$E_\gamma(I \rightarrow I-2)$ (keV)		$J^{(1)}$ ( $\hbar^2\text{MeV}^{-1}$ )		$\hbar^2\omega^2$ ( $\text{MeV}^2$ )	
Exp.[24]	Cal.		Exp.	Cal.	Exp.	Cal.	Exp.	Cal.
99	96.1236	$2^+$	99	96.1236	30.3	31.2098	0.003	0.00307
317	313.6067	$4^+$	218	217.4831	32.1	32.1864	0.013	0.0125
0638	638.4152	$6^+$	321	324.8085	34.25	33.8661	0.026	0.0270
1044	1051.6834	$8^+$	406	413.2682	36.95	36.2960	0.041	0.0426
1520	1532.7315	$10^+$	476	481.0481	39.9	39.4970	0.057	0.0578
2050	2061.2865	$12^+$	530	528.5550	43.4	43.5148	0.070	0.070238
2613	2619.3155	$14^+$	563	558.0290	47.95	48.3845	0.079	0.078169
3191	3193.9583	$16^+$	578	574.6428	53.5	53.9465	0.084	0.082811
3782	3782.4336	$18^+$	591	588.4753	59.0	59.4757	0.087	0.0867878
4408	4395.4460	$20^+$	626	613.0124	62.5	63.6202	0.098	0.094131
5086	5052.8071	$22^+$	678	657.3611	63.5	65.4130	0.115	0.108205
5822	5773.2434	$24^+$	736	720.4363	64.0	65.2382	0.135	0.129933
6613	6568.0523	$26^+$	791	794.8089	64.5	64.1663	0.156	0.1581125
7454	7441.5024	$28^+$	841	873.4501	65.5	62.9686	0.177	0.190917

**Table 3.** The same as Table 2. but for GSRB in  $^{160}\text{Dy}$ .

E (keV)		$I^\pi$	$E_\gamma(I \rightarrow I-2)$ (keV)		$J^{(1)}$ ( $\hbar^2\text{MeV}^{-1}$ )		$\hbar^2\omega^2$ ( $\text{MeV}^2$ )	
Exp.[24]	Cal.		Exp.	Cal.	Exp.	Cal.	Exp.	Cal.
87	85.8606	$2^+$	87	85.8606	34.5	34.9403	0.002	0.002457
284	282.2626	$4^+$	197	196.4020	35.55	35.6411	0.010	0.010233
581	580.7990	$6^+$	297	298.5364	37.05	36.8464	0.022	0.022833
967	969.4982	$8^+$	386	388.6992	38.85	38.5902	0.038	0.03275
1429	1433.9896	$10^+$	462	464.4914	41.15	40.9049	0.053	0.05438
1951	1957.4627	$12^+$	522	523.4731	44.05	43.9373	0.068	0.06889
2515	2518.8105	$14^+$	564	561.3478	47.85	48.0985	0.080	0.0791
3092	3094.5412	$16^+$	577	575.7307	53.72	53.8446	0.083	0.08312
3672	3676.2840	$18^+$	580	581.7428	60.34	60.1640	0.084	0.0848

**Table 4.** The same as Table 2. but for GSRB in  $^{162}\text{Er}$ .

E (keV)		$I^\pi$	$E_\gamma(I \rightarrow I-2)$ (keV)		$J^{(1)}$ ( $\hbar^2\text{MeV}^{-1}$ )		$\hbar^2\omega^2$ ( $\text{MeV}^2$ )	
Exp.[24]	Cal.		Exp.	Cal.	Exp.	Cal.	Exp.	Cal.
102	100.0301	$2^+$	102	100.0301	29.4	29.9909	0.0034	0.00335
330	327.0378	$4^+$	228	227.0077	30.7	30.8359	0.014	0.013671
667	667.7124	$6^+$	337	340.6746	32.65	32.2888	0.029	0.02934
1097	1103.8877	$8^+$	430	436.1753	35.0	34.3898	0.047	0.04819
1603	1614.7940	$10^+$	506	510.9063	37.55	37.1888	0.064	0.06579
2165	2175.2555	$12^+$	562	560.4615	40.95	41.0376	0.079	0.07897
2746	2746.8733	$14^+$	581	571.6178	46.45	47.2343	0.084	0.082022
3292	3296.8214	$16^+$	546	549.9481	57.0	56.3689	0.075	0.07584
3847	3851.4299	$18^+$	555	554.6085	63.0	63.1075	0.077	0.07708
4465	4448.5313	$20^+$	616	597.1014	63.5	65.3155	0.095	0.089308

**Table 5.** The same as Table 2. but for GSRB in  $^{168}\text{Yb}$ .

E (keV)		$I^\pi$	$E_\gamma(I \rightarrow I-2)$ (keV)		$J^{(1)}$ ( $\hbar^2\text{MeV}^{-1}$ )		$\hbar^2\omega^2$ ( $\text{MeV}^2$ )	
Exp.[24]	Cal.		Exp.	Cal.	Exp.	Cal.	Exp.	Cal.
88	87.5156	$2^+$	88	87.5156	34.2	34.2795	0.0026	0.002552
287	286.478	$4^+$	199	198.9624	35.2	35.1825	0.010	0.010502
588	585.998	$6^+$	298	299.5201	36.8	36.7254	0.022	0.02298
970	971.3457	$8^+$	385	385.3476	39.0	38.9258	0.037	0.037618
1425	1426.5171	$10^+$	455	455.1714	41.7	41.7425	0.052	0.05222
1936	1936.4729	$12^+$	511	509.9558	45.05	45.1019	0.065	0.06538
2489	2488.748	$14^+$	553	552.2751	48.85	48.8886	0.076	0.07656
3073	3074.3375	$16^+$	584	585.5895	53.0	52.9381	0.085	0.08599
3687	3687.9627	$18^+$	614	613.6252	57.0	57.0380	0.094	0.09436
4337	4327.9039	$20^+$	650	639.9412	60.0	60.9431	0.106	0.1025

**Table 6.** The same as Table 2. but for GSRB in  $^{170}\text{Yb}$ .

E (keV)		$I^\pi$	$E_\gamma(I \rightarrow I-2)$ (keV)		$J^{(1)}$ ( $\hbar^2\text{MeV}^{-1}$ )		$\hbar^2\omega^2$ ( $\text{MeV}^2$ )	
Exp.[24]	Cal.		Exp.	Cal.	Exp.	Cal.	Exp.	Cal.
84	83.9814	$2^+$	84	83.9814	35.6	35.7221	0.0023	0.0025039
278	277.2103	$4^+$	194	193.2289	36.2	36.2264	0.010	0.0099
573	573.753	$6^+$	295	296.5427	37.2	37.0941	0.022	0.022529
963	964.8507	$8^+$	390	391.0977	38.5	38.3535	0.038	0.03874
1437	1439.4253	$10^+$	474	474.5746	40.1	40.0358	0.056	0.05677
1983	1983.9977	$12^+$	546	544.5724	42.15	42.2349	0.074	0.07456
2580	2581.9719	$14^+$	597	597.9742	45.2	45.1524	0.089	0.08976
3196	3213.8595	$16^+$	616	631.8876	50.5	49.0593	0.095	0.1001
3808	3862.1058	$18^+$	612	648.2463	57.0	53.9918	0.094	0.1053
	4520.3603			658.2545		59.2476		0.10853

**Table 7.** The same as Table 2. but for GSRB in  $^{172}\text{Hf}$ 

9		$I^\pi$	$E_\gamma(I \rightarrow I-2)$ (keV)		$J^{(1)}$ ( $\hbar^2\text{MeV}^{-1}$ )		$\hbar^2\omega^2$ ( $\text{MeV}^2$ )	
Exp.[24]	Cal.		Exp.	Cal.	Exp.	Cal.	Exp.	Cal.
95	94.2326	$2^+$	95	94.2326	31.55	31.8360	0.003	0.002959
309	308.1772	$4^+$	214	213.9446	32.7	32.7187	0.012	0.012143
628	629.434	$6^+$	319	321.2569	34.5	34.2405	0.025	0.02644
1037	1041.1755	$8^+$	409	411.7414	36.7	36.4306	0.042	0.04294
1521	1525.3303	$10^+$	484	484.1548	39.3	39.2436	0.058	0.05908
2065	2065.6671	$12^+$	544	540.3368	42.35	42.5660	0.074	0.0734
2654	2650.1523	$14^+$	589	584.4852	45.8	46.1944	0.087	0.08575
3276	3272.1371	$16^+$	622	621.9848	49.75	49.8404	0.097	0.09701
3918	3930.337	$18^+$	642	658.2000	54.5	53.1753	0.103	0.10857
4575	4627.9229	$20^+$	657	697.5858	59.5	55.9071	0.107	0.1218
5273	5371.1835	$22^+$	698	743.2606	61.5	57.8532	0.121	0.1383

**Table 8.** The same as Table 2. but for GSRB in  $^{174}\text{Hf}$ 

E (keV)		$I^\pi$	$E_\gamma(I \rightarrow I-2)$ (keV)		$J^{(1)}$ ( $\hbar^2\text{MeV}^{-1}$ )		$\hbar^2\omega^2$ ( $\text{MeV}^2$ )	
Exp.[24]	Cal.		Exp.	Cal.	Exp.	Cal.	Exp.	Cal.
91	90.7245	$2^+$	91	90.7245	32.95	33.0671	0.003	0.00274
297	297.3044	$4^+$	206	206.5799	33.9	33.8851	0.011	0.01132
608	609.0077	$6^+$	311	311.7033	35.4	35.2899	0.024	0.02489
1009	1011.0543	$8^+$	401	402.0466	37.4	37.3091	0.040	0.0409
1486	1486.9877	$10^+$	477	475.9334	39.9	39.9215	0.057	0.05709
2020	2020.8607	$12^+$	534	533.8730	43.0	43.0814	0.071	0.07165
2597	2598.9341	$14^+$	577	578.0734	46.85	46.7068	0.083	0.08388
	3210.7221			611.7880		50.6711		0.09386
	3849.4083			638.6862		54.8000		0.10222
	4511.7681			662.3598		58.8803		0.10989
	5197.7693			686.0012		62.6821		0.11784

**Table 9.** The same as Table 2. but for GSRB in  $^{176}\text{Hf}$ 

E (keV)		$I^\pi$	$E_\gamma(I \rightarrow I-2)$ (keV)		$J^{(1)}$ ( $\hbar^2\text{MeV}^{-1}$ )		$\hbar^2\omega^2$ ( $\text{MeV}^2$ )	
Exp.[24]	Cal.		Exp.	Cal.	Exp.	Cal.	Exp.	Cal.
88	88.1506	$2^+$	88	88.1506	33.95	34.0326	0.0025	0.00259
290	290.0005	$4^+$	202	201.8499	34.7	34.6792	0.011	0.0108094
597	597.3852	$6^+$	307	307.3847	35.85	35.7857	0.023	0.02428
998	998.8806	$8^+$	401	401.4954	37.4	37.3603	0.040	0.04083
1481	1481.7119	$10^+$	483	482.8315	39.3	39.3512	0.058	0.05876
2035	2033.868	$12^+$	554	552.1562	41.55	41.6548	0.077	0.07665
2647	2646.048	$14^+$	612	612.1799	44.15	44.1046	0.094	0.09407
3308	3312.9926	$16^+$	661	666.9446	46.85	46.4806	0.109	0.1115
4010	4033.932	$18^+$	702	720.9401	49.85	48.5477	0.123	0.13025
	4812.1773			778.2446		50.1127		0.1517
	5654.1131			841.9358		51.0727		0.1775

The evolution of the traditional kinematic moments of inertia  $J^{(1)}$  as a function of the square of rotational frequency  $\hbar^2\omega^2$  for the ground state rotational bands reported here are illustrated in Figure 1.

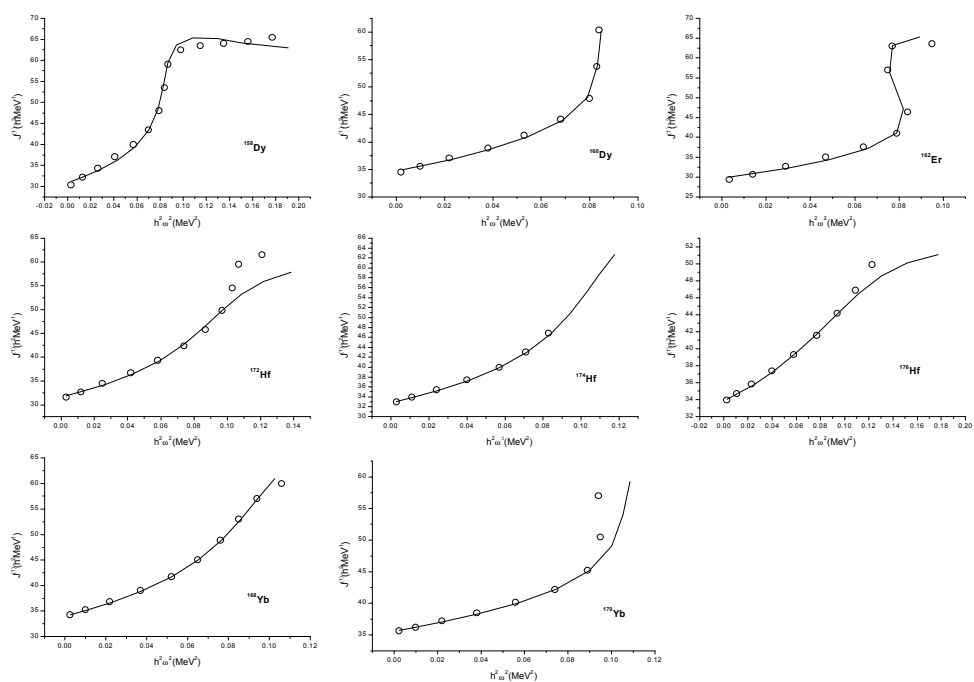


**Figure 1.** The backbending plot of kinematic moments of inertia  $J^{(1)}$  versus the square of rotational frequency  $\hbar^2\omega^2$  for the GSRB of the selected eight nuclei. The parameters used in the level fitting are those given in Table 1. The solid line connects the predictions of one expression. Experimental points are represented by open circles.

Stephens and Simon [3] include nuclei which show explicit backbending in gsb, nuclei exhibiting just upbending in gsb [5]. They also include soft rotor like  $^{158}\text{Dy}$  and good rotor like  $^{160}\text{Dy}$ .

From these figures we notice that the agreement between the calculated and the observed data are excellent.

The present study can also be useful in finding the increase in aligned angular momentum for each band change. In Table 10. and Figure 2. this is done for  $^{162}\text{Er}$ .

**Table 10.** Aligned angular momentum  $i$  as a function of rotational frequency  $\hbar\omega$  for  $^{162}\text{Er}$ . The Harris moment of inertia reference parameters are  $\theta_0 = 28.8\hbar^2\text{MeV}^{-1}$  and  $\theta_1 = 119.0476\hbar^4\text{MeV}^{-3}$ .

$I_i - I_f$ ( $\hbar$ )	$\hbar\omega$ (MeV)		$I_{\text{ref}}$ ( $\hbar$ )		$i$ ( $\hbar$ )	
	Exp.	Cal.	Exp.	Cal.	Exp.	Cal.
2-0	0.0510	0.0500	1.4845	1.4553	0.0154	0.0446
4-2	0.1140	0.1135	3.4599	3.429	0.0404	0.0570
6-4	0.1685	0.1703	5.4223	5.4940	0.0776	0.0059
8-6	0.2150	0.2180	7.3751	7.5157	0.1248	0.0157
10-8	0.2530	0.2554	9.2142	9.3415	0.2857	0.1584
12-10	0.2810	0.2802	10.7342	10.6904	0.7657	0.8095
14-12	0.2905	0.2858	11.2848	11.0106	2.2151	2.4893
16-14	0.2730	0.2749	10.2845	10.3943	5.2154	5.1056
18-16	0.2775	0.2773	10.3359	10.5249	6.9640	6.9750
20-18	0.3080	0.2985	12.3487	11.7661	7.1512	7.7338

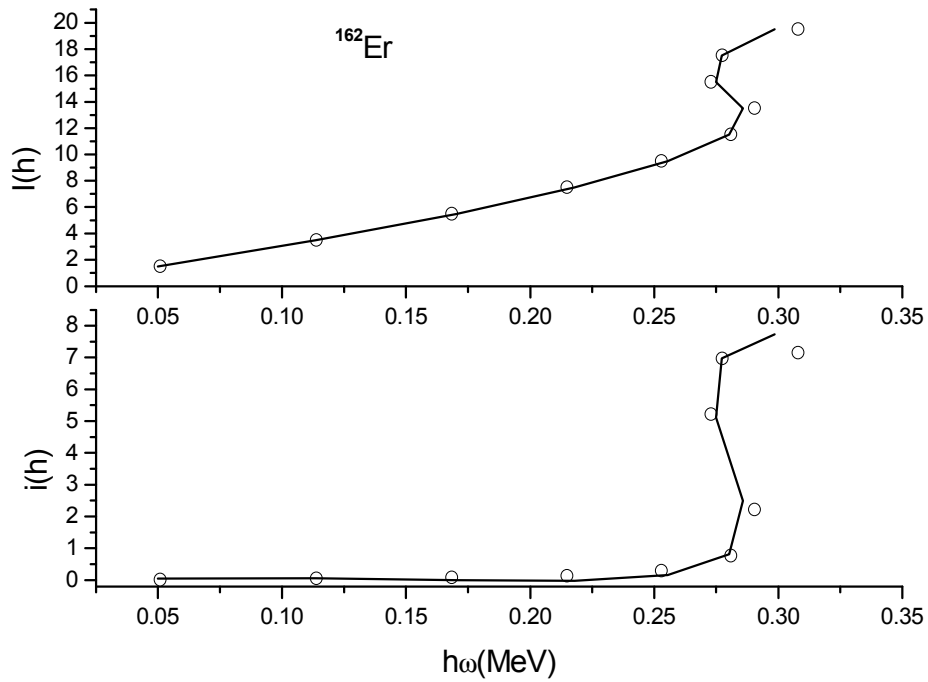


**Figure 2.** Plots of angular momentum  $I$  and increase in aligned angular momentum  $i$  versus rotational frequency  $\hbar\omega$  for  $^{162}\text{Er}$ . The Harris parameters are  $\theta_0 = 28.8\hbar^2\text{MeV}^{-1}$  and  $\theta_1 = 119.0476\hbar^4\text{MeV}^{-3}$ . The solid line indicates the yrast band. The broken line indicates the contribution of the GSRB beyond the band crossing.

In the upper part of the figure a plot of angular momentum versus the rotational frequency is given for both the yrast band and the ground state band. In the lower part of the figure the increase in aligned angular momentum calculated by subtracting the spin of the lower band from that of the upper band at a given frequency versus the rotational frequency is given. It is noticed that an increase at the aligned angular momentum by about 7 units occurs, due to the alignment of a pair of  $i_{13/2}$  neutrons.

## CONCLUSION

Investigating the tables and the figures, we observe that the  $\gamma$ -ray energies and the kinematical moment of inertia of the normal deformed states in the rare-earth region can be quantitatively described with remarkable accuracy, by using our five-parameters simple rotational expression for the moment of inertia. Good agreement is noticed between the calculation using this formula and the observed transition energies which exhibit backbending in rare-earth nuclei including both good and soft rotors.

## REFERENCES

- [1] Johnson, A., Ryde, H. and Sztarkier, *J. Phys. Lett.*, **34B**, 605(1971).
- [2] Mottelson, B.R., and Valatin, J.G., *Phys. Rev. Lett.*, **5**, 511 (1960).
- [3] Stephens, F.S., and Simon, R., *Nucl. Phys.*, **A183**, 257 (1972).
- [4] Molinari, A., and Regge, T., *Phys. Lett.*, **41B**, 93(1972).
- [5] Bengtsson, R., and Frauendorf, S., *Nucl. Phys.*, **A314**, 27(1979), **A327**, 13(1979).
- [6] Bengtsson, R., Hamamoto, I., and Mottelson, B.R., *Phys. Lett.*, **73**, 259(1978).
- [7] Banerjee, B., Mong, I., and Ring, P., *Nucl. Phys.*, **A215**, 36(1973).
- [8] Thieberger, P., *Proceeding Conference On High Spin Nuclear States and Related Phenomena*, Stockholm, Sweden, May 30 - June 3, 1972.
- [9] Thieberger, P., *Phys. Lett.*, **45B**, 41(1973).
- [10] Smith, B.C., and Volkov, A.B., *Phys. Lett.*, **47B**, 143(1973).
- [11] Walker, P.M., et al., *Phys. Lett.*, **B309**, 14(1993).
- [12] Kutsarova, T., et al., *Nucl. Phys.*, **A587**, 11(1995).
- [13] Shizuma, T., et al., *Nucl. Phys.*, **A593**, 247(1995).
- [14] Shizuma, T., et al., *Phys. Lett.*, **B442**, 53(1998).
- [15] Walker, P.M., *Proceeding of the International Conference on the Future for Nuclear Spectroscopy*, Crete, 1993.
- [16] Frauendorf, S., *Nucl. Phys.*, **A557**, 259C(1993).
- [17] Cescato, M.L., Sun, Y., and Ring, R., *Nucl. Phys.*, **A533**, 45(1991).
- [18] Velazquez, V., et al., *Nucl. Phys.*, **A 653**, 355(1999).

- [19] Cwick,S., et al., *Phys. Rev.*, **C21**, 448(1980).  
 [20] Zeng,J.Y., Jin,T.I., and Zhao,Z.I., *Phys. Rev.*, **C50**, 1388(1994).  
 [21] Mariscotti,M.A.J., Scharf-Goldhaber ,G.,and Buch,B., *Phys. Rev.*, **178**, 1864(1969).  
 [22] Scharf Goldhaber,G., Doner,C.B., and Goodman, A.L., *Ann. Rev. Nucl. Sc.*, **26**, 230(1976).  
 [23] Harris,S.M., *Phys. Rev.*, **138**, 500(1965).  
 [24] Atomic Data and Nuclear Data Tables, 52 (1992).

## وصف الحزم الدورانية عند غزل عالي للأنوية الأرضية النادرة الزوجية باستخدام صيغة متعددة البارامترات لعزم القصور الذاتي الكيناميتيكي

منال محمود سراج

قسم الفيزياء - كلية البنات للآداب والعلوم والتربية - جامعة عين شمس

حيث أن شكل العلاقة بين عزم القصور الذاتي مع مربع التردد الدوراني يعطى التفاصيل للطيف النووي الدوراني ، فإنه من المفضل استخدام عزم القصور الذاتي بدلا من استخدام الطاقات للدراسة. استخدمت كثيرة الحدود المتعددة البارامترات ذات القوى الزوجية في كمية التحرك الزاوية المتوسطة لعزم القصور الذاتي الكيناميتيكي لتحليل حزم المستويات الدورانية ذات أقل طاقة للأنوية المشوهة الزوجية-الزوجية في منطقة العناصر الأرضية النادرة عند غزل عالي. اشتقت البارامترات المثلى ببرنامج باحث باستخدام الحاسب لجعل مربع الجذر التربيعي لفروق عزوم القصور الذاتي الكيناميتيكي النظري والتجريبي أقل ما يمكن. استخدمت الصيغة متعددة البارامترات لتحقيق حدوث الانحناء للخلف والانحناء لأعلى في عزوم القصور الذاتي النووي. وتم في هذا البحث دراسة لتركيب مستويات الطاقة حتى غزل  $20^+$  لثمانية أنوية ذات دوار لين ودوار جيد وذات انحناء للخلف أو انحناء لأعلى.